FRONTIERS OF PHYSICS

RESEARCH ARTICLE
Volume 18 / Issue 1 / 12305 / 2023

Spinning microresonator-induced chiral optical transmission

Lu Bo[1], Xiao-Fei Liu[1,†], Chuan Wang[2], Tie-Jun Wang[1,‡]

1 State Key Laboratory of Information Photonics and Optical Communications and School of Science, Beijing University of Posts and Telecommunications, Beijing 100876, China
2 School of Artificial Intelligence, Beijing Normal University, Beijing 100875, China
Corresponding authors. E-mail: †xfeiliu@163.com, ‡wangtiejun@bupt.edu.cn
Received June 10, 2022; accepted October 12, 2022

ABSTRACT

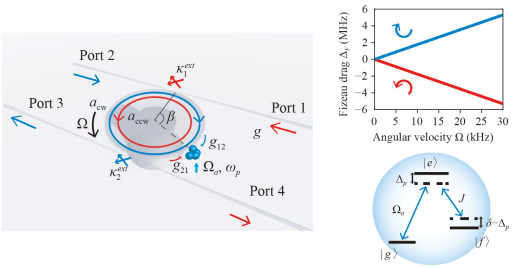

Chiral quantum optics is a new research area in light-matter interaction that depends on the direction of light propagation and offers a new path for the quantum regulation of light-matter interactions. In this paper, we study a spinning Kerr-type microresonator coupled with Λ-type atom ensembles, which are driven in opposite directions to generate asymmetric photon statistics. We find that a photon blockade can only be generated by driving the spinning resonator on right side without driving the spinning microresonator from the left side, resulting in chirality. The coupling strength between system modes can be precisely controlled by adjusting the detuning amount of the atomic pump field. Because of the splitting of the resonant frequency generated by the Fizeau drag, the destructive quantum interference generated in right side drive prevents the nonresonant transition path of state $|1,0\rangle$ to state $|2,0\rangle$. This direction-dependent chiral quantum optics is expected to be applied to chiral optical devices, single-photon sources and nonreciprocal quantum communications.

Keywords chiral quantum optics, spinning microresonator, nonreciprocal, photon blockade

1 Introduction

Chirality is a special symmetry of existence in nature that describes the mirror-symmetry property of a system. It has received widespread attention and is involved in many physical phenomena, such as the quantum Hall effect [1], topological insulators [2, 3], and superconductors [4]. In advanced photonics nanostructured devices [5–11], strong light confinement can lock the local polarization of light in its propagation direction, which causes the emission, scattering, and absorption of photons by the quantum emitter to depend on the propagation direction. This research field, which depends on the propagation direction, that is, chirality combined with quantum optics, is called chiral quantum optics [12]. In chiral quantum optics, the result of light–matter interactions depends on the propagation of light; that is, forward and backward propagating photons and matter will have different interactions. Consequently, the light–matter interaction becomes nonreciprocal, and even photon blockades occur under extreme conditions.

Chiral quantum optics are widely used in photonic nanostructured devices, such as photonic waveguides that restrict the propagation direction [7], one-dimensional quantum emitters based on chiral coupling [13], and spin-momentum-locked light coupled to quantum emitters with polarization-dependent dipole transitions [14–17]. There are many methods used to achieve chiral optics, such as breaking the parity–time (PT) symmetry of the system to achieve nonreciprocality [18–20], chiral coupling of Rydberg atoms with microcavities [8, 13], using a nonlinear Kerr-type microcavity [21–23],

Higher Education Press

https://doi.org/10.1007/s11467-022-1212-z

optomagnonics [24–26], and using optomechanical devices [27–30]. Microcavities are an excellent way to achieve chiral quantum optics, as they greatly enhance light–matter interactions. In recent years, there have been significant advances in experimental microcavities with small mode volumes on the microscale and ultra-high-quality factor Q ($\sim 10^8$), which can greatly improve the performance of light–matter interactions [31–35]. They have been widely used in optomechanics [36–41], nonlinear optics [42–44], PT symmetric or antisymmetric optics [19, 45–47], cavity quantum electrodynamics (C-QED) [48], and ultrasensitive detection [49–53].

In particular, a spinning microresonator splits the resonant frequency of the countercirculating modes due to the Fizeau drag. In a recent experiment [54], based on the optical Sagnac effect, 99.6% optical isolation was achieved in a spinning resonator. There has been considerable research on microresonators because they can produce photon blockades (PBs) and thus play an important role in achieving nonreciprocal single photon sources, which are crucial elements for quantum information [55–58]. Moreover, by adjusting the amount of detuning and the rotation speed of the resonator, the chiral light–matter interaction has a high degree of controllability and good application prospects in quantum information processing. Meanwhile, symmetric mode-coupled nanoparticle-enhanced sensing by spinning microresonators has also been proposed [57]. However, this requirement that controlling coupling strength depending on nanoparticle location is difficult. Due to the characteristics of chiral quantum optics, we expect to obtain a chiral optical system with adjustable optical mode coupling strength in the resonator. Fortunately, we can adjust the atom-cavity mode coupling strength by adjusting the frequency and strength of the external control field [8].

In this paper, we demonstrate a precisely adjustable chiral optical system composed of a spinning Kerr-type resonator and Λ-type atom ensembles. We can control the chirality of the system by changing the coupling strength between modes, the rotation speed of the resonator, and detuning amount of the light field. We find that destructive quantum interference between different excitation levels results in chirality even under weaker nonlinear conditions; that is, a photon blockade can only be produced by right side of the drive device and not left side. Our work can be used as a new method for realizing chiral optical devices, single-photon sources and nonreciprocal quantum communication.

2 The physical model and solution

The system considered here is a spinning resonator coupled with an add-drop-type taper fiber and a single three-level atom ensemble, as shown in Fig. 1(a). The spinning resonator rotates at angular velocity Ω and supports both clockwise (CW) and counterclockwise (CCW) optical modes (with the same frequency ω_c and dissipation rate κ). The light circulating in the resonator changes the Fizeau drag due to rotation, and the relationship between the Fizeau drag and the detuning amount is shown in Fig. 1(b), i.e., $\omega_0 \to \omega_0 + \Delta_F$, with [59]

$$\Delta_F = \pm\frac{nr\Omega\omega_0}{c}\left(1-\frac{1}{n^2}-\frac{\lambda}{n}\frac{\mathrm{d}n}{\mathrm{d}\lambda}\right) = \pm\eta\Omega, \tag{1}$$

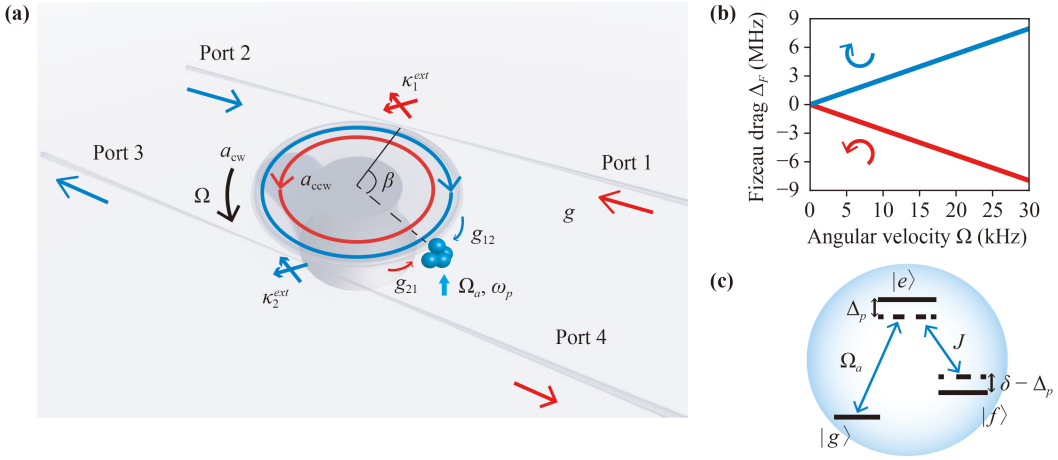

Fig. 1 **(a)** Illustration of a spinning resonator coupled atom ensemble. The spinning resonator rotates counterclockwise at angular velocity Ω, and both CW and CCW modes are excited simultaneously in the microcavity. When a probe signal is input from port 1 (or port 2) or a transmission is detected from port 4 (or port 3), the intrinsic dissipation of the resonator is κ_0, and the dissipation of coupling with the fibers on both sides is κ_1^{ext} and κ_2^{ext}. **(b)** Fizeau drag Δ_F versus angular velocity Ω of the resonator for the CCW (red line) and CW (blue line) cases. **(c)** The Λ-type energy level of the atom and its interaction with the cavity mode and external control field. The parameters are as follows: the optical wavelength is $\lambda = 1550$ nm, the radius of the resonator is $r = 100$ μm, the coupling strength between cavity modes (CW and CCW) is J, and the linear refractive index of the resonator is $n = 1.4$.

where ω_0 is the resonance frequency of a nonspinning resonator, n is the refractive index, r is the resonator radius, $c(\lambda)$ is the speed (wavelength) of light in vacuum, and the dispersion term $\mathrm{d}n/\mathrm{d}\lambda$, characterizing the relativistic origin of the Sagnac effect, is relatively small. Therefore, in our model, where the resonator rotates counterclockwise, the CW mode exists at $\Delta_F > 0$, and the CCW mode exists at $\Delta_F < 0$. Fig. 1(c) shows the Λ-type energy levels of the atom, in which $|e^k\rangle \leftrightarrow |g^k\rangle$ represents the k-th atom transformation in the ensemble, and the transition is driven by an external control field with central frequency ω_p. Because Δ_F brought by the Fizeau drag is much smaller than ω_c, we assume that the $|e^k\rangle \leftrightarrow |f^k\rangle$ transition can simultaneously interact with the degenerate CW and CCW modes with the same coupling strength J, drive strength Ω_a and phase β. By switching off the beam and magnetic field of the magneto-optical trap (MOT) that traps ultracold atoms, we can make a few atoms fall from fixed positions to the microresonator and the coupling strength of which can be regarded as constant.

We consider the case where the resonator is driven on the right (or left) when the probe signal is input from port 1 (or port 2) or the transmission is detected from port 4 (or port 3). The Hamiltonian of the system driven by a weak laser on the left side can be described as $\hat{H} = \hat{H}_c + \hat{H}_a + \hat{H}_I$. $\hat{H}_c$ denotes the Hamiltonian of the resonator, which is $\hat{H}_c = (\omega_c - \Delta_F)\hat{a}^\dagger_{cw}\hat{a}_{cw} + (\omega_c + \Delta_F)\hat{a}^\dagger_{ccw}\hat{a}_{ccw}$ by setting $\hbar = 1$. The Hamiltonian of the Λ-type energy level atom ensemble coupled to the resonator is $\hat{H}_a = \Sigma_k(\omega_e\sigma^k_{ee} + \omega_g\sigma^k_{gg} + \omega_f\sigma^k_{ff})$, and $\sigma^k_{ii} = |i^k\rangle\langle i^k|$ stands for the corresponding transitions. The Hamiltonian $\hat{H}_I$ of the interaction between the atom and the light field can be expressed as

$$\hat{H}_I = \Sigma_k[J\sigma^k_{ef}(\hat{a}_{cw}\mathrm{e}^{\mathrm{i}\beta} + \hat{a}_{ccw}\mathrm{e}^{-\mathrm{i}\beta}) + \Omega_a\sigma^k_{eg}\mathrm{e}^{-\mathrm{i}\omega_p t} + H.c.], \tag{2}$$

where $\sigma^k_{ef} = |e^k\rangle\langle f^k|$ corresponds to the k-th atom in ensemble transitions from $|e^k\rangle$ to $|f^k\rangle$, and the creation $\hat{a}^\dagger_{cw}$ ($\hat{a}^\dagger_{ccw}$) and the annihilation operator $\hat{a}_{cw}$ ($\hat{a}_{ccw}$) are the bosonic operators of the cavity CW mode and CCW mode.

When the effective detunings are much larger than the corresponding coupling strength ($\delta, \Delta_p \gg J, \Omega_a$) and the atom ensemble detuning Δ_a and the dissipation γ are larger than those of optical modes ($\Delta_a, \gamma \gg \Delta_c, \kappa$), the excited states can be adiabatically eliminated. Considering the dissipation and the nonlinear term of this system, the effective Hamiltonian is non-Hermitian, which can be expressed as [8]

$$\begin{aligned}\hat{H}_{eff} =& \mathrm{i}\chi G^2\mathrm{e}^{-\mathrm{i}2\beta}\hat{a}^\dagger_{cw}\hat{a}_{ccw} + \mathrm{i}\chi G^2\mathrm{e}^{\mathrm{i}2\beta}\hat{a}_{cw}\hat{a}^\dagger_{ccw} \\ &+ (\Delta_{cw} - \mathrm{i}\frac{\kappa'}{2})\hat{a}^\dagger_{cw}\hat{a}_{cw} + \left(\Delta_{ccw} - \mathrm{i}\frac{\kappa'}{2}\right)\hat{a}^\dagger_{ccw}\hat{a}_{ccw}.\end{aligned} \tag{3}$$

Here, $G = \Omega_a J/\Delta_p$, $\chi = 4\mathrm{i}(\Delta_a - J^2/\Delta_p)/\gamma^2 - 4/\gamma$, and $\Delta_{cw(ccw)} = \Delta_c \mp \Delta_F - G^2\Delta_a/(\Delta_a^2 + \gamma^2/4)$. The effective detuning of the atomic and cavity mode pump fields is $\Delta_a = \omega_p + \omega_g - \omega_f + \Omega_a^2/\Delta_p^2 - \omega_c^i n$, and the dissipation of optical modes is $\kappa' = \kappa + G^2\gamma/(\Delta_a^2 + \gamma^2/4)$. Therefore, we can change the coupling strength between the optical mode $\hat{a}_{cw}$ and $\hat{a}_{ccw}$ by changing the Rabi frequency Ω_a and the detuning ω_p of the atom ensemble, avoiding the difficulty of adjusting the nanoscale atom ensemble's position.

Consider the Kerr nonlinear terms $\hat{a}^\dagger_{ccw}\hat{a}^\dagger_{ccw}\hat{a}_{ccw}\hat{a}_{ccw}$ and $\hat{a}^\dagger_{cw}\hat{a}^\dagger_{cw}\hat{a}_{cw}\hat{a}_{cw}$ and the cross Kerr nonlinear term $\hat{a}^\dagger_{cw}\hat{a}_{cw}\hat{a}^\dagger_{ccw}\hat{a}_{ccw}$ that exist in the system. The cross Kerr nonlinear term is related to the quadratic term of J, after adiabatic elimination of atom. Under $\gamma \gg \Delta_a$, the Taylor series expansion of $\chi = \frac{4}{\gamma^2}[\mathrm{i}\Delta_a - \mathrm{i}J^2/\Delta_p - \gamma]$ yields the nonlinear Kerr terms and the cross Kerr nonlinear term. At this moment, the effective Hamiltonian of the system can be written as $\hat{H} = \hat{H}_0 + \hat{H}_s + \hat{H}_d$. Where $\hat{H}_0 = \Delta_{cw}\hat{a}^\dagger_{cw}\hat{a}_{cw} + \Delta_{ccw}\hat{a}^\dagger_{ccw}\hat{a}_{ccw} + U(\hat{a}^\dagger_{cw}\hat{a}^\dagger_{cw}\hat{a}_{cw}\hat{a}_{cw} + \hat{a}^\dagger_{ccw}\hat{a}^\dagger_{ccw}\hat{a}_{ccw}\hat{a}_{ccw})$, $\hat{H}_s = g_{12}\hat{a}^\dagger_{cw}\hat{a}_{ccw} + g_{21}\hat{a}^\dagger_{ccw}\hat{a}_{cw} + 2U\hat{a}^\dagger_{cw}\hat{a}_{cw}\hat{a}^\dagger_{ccw}\hat{a}_{ccw}$, and $\hat{H}_d = \varepsilon(\hat{a}^\dagger_{cw} + \hat{a}_{cw})$. Here, the nonlinear term U is $-4G^2J^2/(\gamma^2\Delta_p)$, while the asymmetric coupling terms are $g_{12} = 4\mathrm{i}G^2(\mathrm{i}\Delta_a - \gamma)\mathrm{e}^{-\mathrm{i}2\beta}/\gamma^2$ and $g_{21} = 4\mathrm{i}G^2(\mathrm{i}\Delta_a - \gamma)\mathrm{e}^{\mathrm{i}2\beta}/\gamma^2$. And $g_{12} = g_{21} = g$ when the phase of the atoms is the same $\beta = 0$. When the excitation of the optical mode is weak enough, only lower excited states can be excited, and the average number of photons in the microcavity is relatively small. Assuming that the maximum number of photons is less than 2, the state of this system becomes

$$\begin{aligned}|\varphi\rangle =& C_{00}|00\rangle + C_{10}|10\rangle + C_{01}|01\rangle \\ &+ C_{20}|20\rangle + C_{02}|02\rangle + C_{11}|11\rangle,\end{aligned} \tag{4}$$

where $|n_{cw}, n_{ccw}\rangle$ represents the Fock state in which this system has n_{cw} photons in the CW mode and n_{ccw} photons in the CCW mode. Due to the weak driving condition, we have $C_{00} \gg C_{10}, C_{01} \gg C_{11}, C_{20}, C_{02}$. Wave function evolution satisfies the Schrödinger equation, and we obtain the dynamic equations for the coefficients $C_{cw,ccw}$.

First, we consider the one-photon excitation states. The evolution of these two states can be described as

$$\mathrm{i}\frac{\partial C_{10}}{\partial t} = (\Delta' - \Delta_F - \mathrm{i}\kappa/2)C_{10} + gC_{01} + \varepsilon C_{00}, \tag{5}$$

$$\mathrm{i}\frac{\partial C_{01}}{\partial t} = (\Delta' + \Delta_F - \mathrm{i}\kappa/2)C_{01} + gC_{10}. \tag{6}$$

Here $\Delta' = \Delta_c - G^2\Delta_a/(\Delta_a^2 + \gamma^2/4)$. Using steady-state conditions, we obtain $C_{01} = -g\Xi_2 C_{10}$, where $\Xi_2^{-1} = \Delta' + \Delta_F - \mathrm{i}\kappa/2$ and

$$C_{10} = \frac{\varepsilon C_{00}}{\Xi_0^{-1} - g^2\Xi_2}, \tag{7}$$

where $\Xi_0^{-1} = \Delta' - \Delta_F + i\kappa/2$. Next, we consider the evolution of two-photon excitation states, and the evolution of these states can be given by the Schrödinger equation

$$i\frac{\partial C_{20}}{\partial t} = (2\Delta' - \Delta_F - i\kappa + 2U)C_{20} + \sqrt{2}\varepsilon C_{10} + \sqrt{2}gC_{11}, \quad (8)$$

$$i\frac{\partial C_{11}}{\partial t} = (2\Delta' - i\kappa + 2U)C_{11} + \sqrt{2}gC_{02} + \varepsilon C_{01} + \sqrt{2}gC_{20}, \quad (9)$$

$$i\frac{\partial C_{02}}{\partial t} = (2\Delta' + \Delta_F - i\kappa + 2U)C_{02} + \sqrt{2}gC_{11}. \quad (10)$$

Under adiabatic evolution, we have $\frac{\partial C_{02}}{\partial t} = 0$ in the steady-state situation. Therefore, we obtain $2C_{02} = -\sqrt{2}g\Xi_2' C_{11}$, $\Xi_2^{'-1} = \Delta' + \Delta_F - i\kappa/2 + U$. Taking this formula into Eqs. (8) and (9) and using steady-state conditions, we have

$$0 = 2\Xi_0^{'-1}C_{20} + \sqrt{2}\varepsilon C_{10} + \sqrt{2}gC_{11}, \quad (11)$$

$$0 = (2\Xi_1^{'-1} - g^2\Xi_2')C_{11} + \sqrt{2}gC_{20} + \varepsilon g\Xi_2 C_{10}. \quad (12)$$

From Eqs. (11) and (12), we obtain

$$C_{11} = \frac{\varepsilon g\Xi_2 + \varepsilon g\Xi_0}{2\Xi_1^{'-1} - g^2\Xi_2' - g^2\Xi_0'}C_{10}, \quad (13)$$

$$C_{20} = \left(\frac{1}{\sqrt{2}}\right)\frac{2\Xi_0'\Xi_1^{'-1} + g^2(\Xi_2 + \Xi_2')\Xi_0'}{2\Xi_1^{'-1} - g^2\Xi_2' - g^2\Xi_0'}\varepsilon C_{10}, \quad (14)$$

where $\Xi_1^{'-1} = \Delta' - i\kappa/2 + U$ and $\Xi_0^{'-1} = \Delta' - \Delta_F - i\kappa/2 + U$.

In this paper, we mainly study the influence of the spin direction and velocity of the resonator on the statistical properties of the system photons. Therefore, we use the second-order correlation function $g^{(2)}(0)$ to measure the statistical properties of photons. In the steady state, the second-order correlation function is expressed as

$$g_L^{(2)}(0) = \frac{\langle \hat{a}_{cw}^\dagger \hat{a}_{cw}^\dagger \hat{a}_{cw}\hat{a}_{cw}\rangle}{\langle \hat{a}_{cw}^\dagger \hat{a}_{cw}\rangle^2}. \quad (15)$$

Due to a weak pump, we obtain $C_{00} \gg C_{01}, C_{10} \sim \varepsilon \gg C_{02}, C_{20}, C_{11} \sim \varepsilon^2$. We denote the probability of finding $|n_{cw}, n_{ccw}\rangle$ in the resonator by $P_{cw,ccw} = |C_{cw,ccw}|^2$. Then, we approximate $g_L^{(2)}(0) \simeq \frac{2|C_{20}|^2}{|C_{10}|^4}$.

3 Chiral light–matter interaction

In this section, we present an analysis of the various parameters of the second-order correlation function $g_L^{(2)}$ ($g_R^{(2)}$). We assume a sufficiently weak drive field ($\varepsilon = 0.01\kappa$) so that the number of photons in the microcavity is small enough for photon blockade. For convenience, we normalize all the parameters to the dissipation rate of the cavity modes κ.

We have realized a system of three-level atoms coupled with a microcavity with adjustable coupling strength between optical modes. Therefore, we studied the relationship between the coupling strength g_{12} and the second-order coherence functions $g^{(2)}(0)$ when the effective detuning amount is 0 and $\Omega = 5$ kHz, as shown in Fig. 2(a). We find that with increasing coupling strength, the second-order coherence function $g^{(2)}(0)$ first decreases and then increases. Therefore, we can choose the appropriate coupling strength to achieve photon blockage. To understand the relationship between the

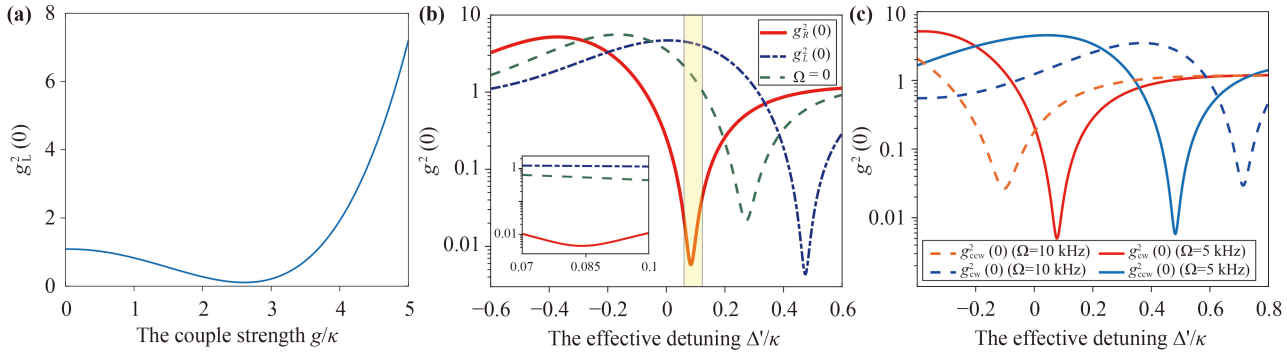

Fig. 2 Equal-time second-order correlation functions $g^{(2)}(0)$ as functions of the couple strength, detuning Δ, and rotation speed Ω. **(a)** The change in second-order coherence functions $g_L^{(2)}(0)$ with coupling strength when the system is driven on the left. **(b)** The change in second-order correlation functions $g^{(2)}(0)$ with the effective detuning Δ'/κ under different driving directions. At $\Delta/\kappa \simeq 0.085$, by driving the resonator on the left or right side, different properties will appear, with the right side driving for photon blockade and the left side for photon bunching. A nonspinning resonator is represented by a green line. **(c)** The second-order correlation functions $g^{(2)}(0)$ plotted as functions of the rotation speed Ω. The blue and red solid lines represent $g^{(2)}(0)$ of the system driven by the left and the right when $\Omega = 5$ kHz, and the dotted line represents the case of $\Omega = 10$ kHz. The parameters are chosen as the coupling strength g_{12} and $g_{21} = 3\kappa$, $\varepsilon = 0.01\kappa$, $n = 1.4$, $r = 100$ μm, $Q = 2.5 \times 10^8$, $\Omega = 5$ kHz ($\Delta_F/\kappa = 0.3$), $\kappa = 5$ MHz, $U = 0.05\kappa$ and $\lambda = 1550$ nm.

photon statistical properties of the spinning resonator and the driving direction. We show the logarithmic plot (of base 10) of the equal-time second-order correlation functions $g^{(2)}(0)$ as functions of the effective detuning Δ'/κ and the rotation speed Ω in Fig. 2. We show the equal-time second-order correlation functions $g^{(2)}(0)$ plotted as functions of the detuning Δ/κ in Fig. 2(b) for $U = 0.05\kappa$, $|g| = 3\kappa$, and resonator spinning speed $\Omega = 5k$Hz. We find that $g^{(2)}(0)$ driven by different sides are very different even under the same amount of detuning (i.e., $g_R^{(2)}(0) \ll 1$ at $\Delta'/\kappa \simeq 0.085$, while $g_L^{(2)}(0) > 1$ at $\Delta'/\kappa \simeq 0.085$). These results indicate that the photons on the left-hand drive system ($\Delta'/\kappa \simeq 0.085$) exhibit the effect of a photon blockade (a photon enters the resonator and blocks subsequent photon entry). The system under the same conditions ($\Delta'/\kappa \simeq 0.085$) is driven on the right side, and photons exhibit photon bunching (a photon enters the resonator and induces subsequent photon entry). For a nonspinning resonator, $g^{(2)}(0)$ always has a dip at $\Delta'/\kappa \simeq 0.3$ or peak at $\Delta'/\kappa \simeq -0.19$. We obtain results that the points for the strong antibunching numerically drift due to the Fizeau shift of the resonator spinning relative to the resonator without spinning, similar to the Doppler effect with Fig. 2. Moreover, we also show the change in $g^{(2)}(0)$ with rotation speed Ω in Fig. 2(c). We find that as the rotation speed increases, the image of $g^{(2)}(0)$ drifts toward the direction of increased detuning.

To show the influence of the input light direction on the statistical characteristics of the system photon, that is, whether the chiral effect is obvious, we introduce the chiral parameter

$$\Gamma = \frac{g_L^{(2)}(0) - g_R^{(2)}(0)}{g_L^{(2)}(0) + g_R^{(2)}(0)}. \tag{16}$$

The parameter Γ versus the spinning speed Ω and the effective detuning Δ'/κ are shown in Fig. 3(a). When $g_L^{(2)}(0)$ (or $g_R^{(2)}(0)$) becomes zero, the chirality becomes 1 (or –1). In other words, when $g_L^{(2)}(0) = 0$ (or $g_R^{(2)}(0) = 0$), the system excited by the left side (right side) is in photon blockade, and we can think of it as a system with a strong chiral effect. Chirality generation is the cleft of the cavity mode by the Fizeau shift Δ_F generated by the spinning resonator. Photons are easily generated by excitation on the right side and suppressed by excitation on the left side in the blue highlighted area. A photon blockade can be simplified by changing the driving direction. We can obtain a chirality photon blockade by changing the spinning speed Ω of the spinning resonator and the effective detuning Δ'/κ.

To obtain a system with the largest chiral value, the photon statistical property of driving on the right side is a photon blockade, and driving on the left side is a photon bunching. We give the relationship between the second-order correlation function of the left-hand drive and the right-hand drive at the same spinning speed of the resonator and the amount of detuning in Fig. 3(b). We find that as the amount of detuning increases, the spinning speed Ω required to satisfy the optimal condition points of the systems driven on the right side and left side shifts in the opposite direction. In Fig. 3(b), we find that a system with a strong chiral effect can be obtained at a specific detuning and spinning speed, and the chiral effect disappears when the spinning speed is very small.

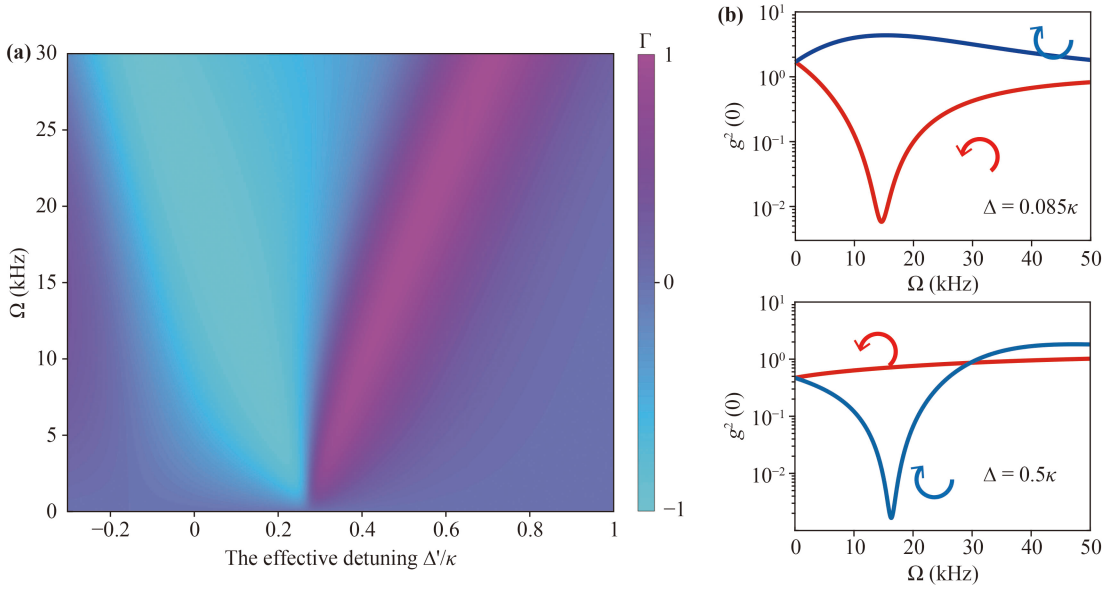

Fig. 3 **(a)** Dependence of parameter Γ on the effective detuning Δ'/κ and the spinning speed Ω. Other parameters, the nonlinear interaction strength $U/\kappa = 0.05$ and the coupling strength $|g| = 3\kappa$. **(b)** The equal-time second-order correlation functions $g^{(2)}(0)$ as functions of the spinning speed Ω. Other parameters are consistent with (a), and the amount of detuning increases from top to bottom. The red and blue lines are driven on the right side and left side, respectively.

By adjusting the amount of detuning and the spinning speed of the resonator, we can obtain a system with a strong chiral effect.

4 Optimal parameters for photon blockade

In this section, we analytically drive the optimal conditions of a photo blockade. Previous studies have shown destructive quantum interference effects between different optical modes, so two coupled quantum modes with weak nonlinearity can be used as a single photon source [60, 61]. To date, more photon blockade properties in coupled-mode systems have been studied by theory and experimentation. Our system consists of optical modes with Kerr nonlinearity, which can also achieve unconventional photon blockades based on the results of previous studies. A chiral rotating microresonator can be used as a single photon source in the case of a photon blockade (PB) (i.e., $g_L^2(0)=0$). From Eqs. (8)–(10) and setting C_{20} to approach zero, we obtain the optimal condition equation as

$$\begin{vmatrix} 0 & g_{12} & \varepsilon \\ \sqrt{2}\Xi_2^{'-1} & g_{21} & 0 \\ \sqrt{2}g & 2\Xi_1^{'-1} & -\varepsilon g \Xi_2 \end{vmatrix} = 0, \tag{17}$$

or

$$\begin{aligned} &2U^2(\Delta'+\Delta_F)+U(g_{12}g_{21}-\kappa'^2+4\Delta'^2+6\Delta'\Delta_F+2\Delta_F^2) \\ &+2\Delta'(\Delta'+\Delta_F)^2-\left(\frac{3\Delta'}{2}+\Delta_F\right)\kappa'^2-\mathrm{i}U\kappa'(4\Delta'+3\Delta_F) \\ &-\mathrm{i}U^2\kappa'-\mathrm{i}\kappa'(3\Delta'+\Delta_F)(\Delta'+\Delta_F)+\mathrm{i}\frac{\kappa'^3}{4}=0. \end{aligned} \tag{18}$$

As the Kerr nonlinearity U is weak enough to ignore the second-order term, the amount of detuning should be satisfied under the optimal solution,

$$\Delta_{opt} \simeq -\frac{2}{3}\Delta_F \pm \frac{\kappa'}{2\sqrt{3}}, \tag{19}$$

$$U_{opt} \simeq \pm\frac{2}{\sqrt{3}}\frac{\kappa'^3}{3g^2-2\kappa'^2}. \tag{20}$$

The change in $g_L^{(2)}(0)$ with the coupling strength $|g_{12}|$ (or $|g_{21}|$) and the Kerr nonlinearity U is shown in Fig. 4. It can be observed that as g increases, the optimal U_{opt}

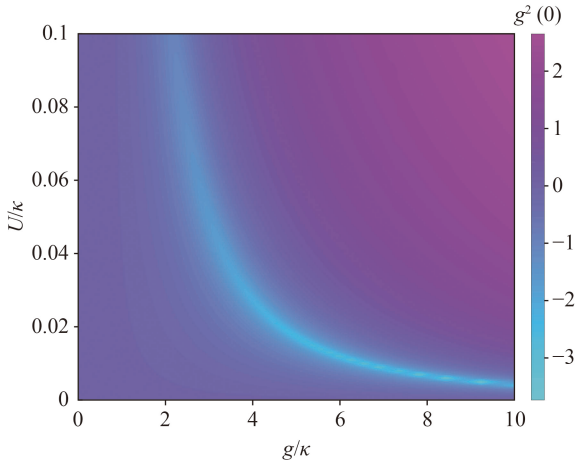

Fig. 4 The changes of the equal-time second-order correlation function $g_L^{(2)}0$ as the coupling strength g with the Kerr nonlinearity U. The marked line is the optical U_{opt} calculated from above. The detuning Δ is chosen as 0.105κ. The values of the other parameters are $\varepsilon=0.01\kappa$ and $\Delta_F=0.3\kappa$.

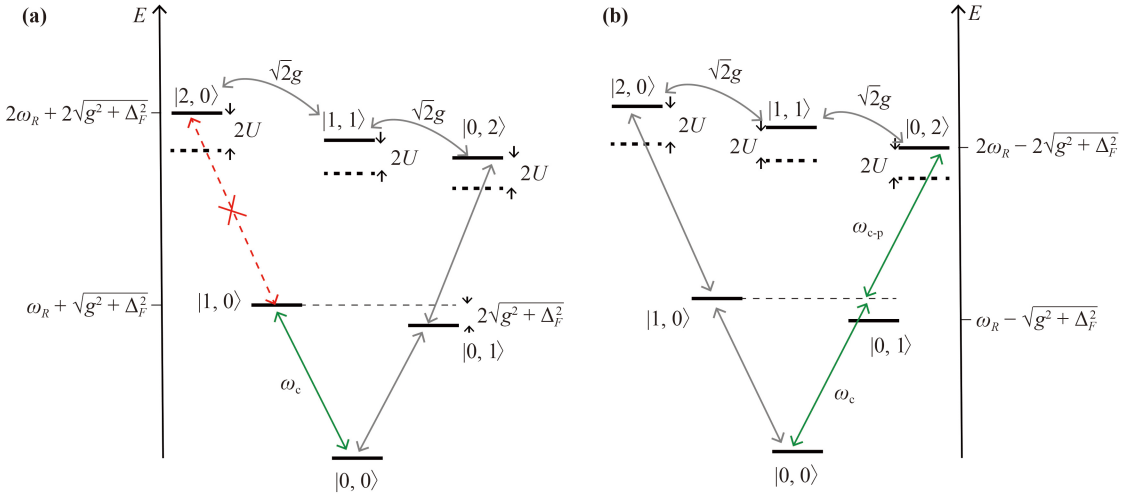

Fig. 5 The energy level diagram shows the zero-photon, single-photon and two-photon states and transition path leading to quantum interference responsible for the photon blockade (the solid green line with arrows is the transition path that is allowed to occur, the dashed red line is the transition path that is not allowed to occur, and the gray lines indicate quantum transition pathways with interference). **(a)** and **(b)** represent the photon blockade from the right drive and the photon bunching caused by the left drive, respectively.

required for the minimum of $g_{cw}^{(2)}(0)$ decreases simultaneously. In other words, we can increase the coupling strength g in the experiment to reduce the required nonlinear Kerr term U. As noted above, an increase in g enhances quantum interference between different states and thus enhances the photon blockade effect.

We show the energy-level diagram and the transition paths in Fig. 5. We can get the eigenenergy of the supermodel $\omega_{\pm} = \omega_R \pm \sqrt{g^2 + \Delta_F}$ from Eq. (4). When $U = 2\sqrt{g^2 + \Delta_F}$, the energy of the left-driven system just satisfies the single-photon excitation, and the detuning of $2U$ suppresses the further transition of the photon, resulting in photon blockade. Meanwhile, the left-driven system just satisfies the two-photon resonance, resulting in photon-induced tunneling (PIT). In the quantum transition pathway, the optimal nonlinear interaction strength is inversely proportional to the coupling strength when $\Delta = \Delta_{opt}$, and the increase in coupling strength results in the suppression of the nonresonant transition from state $|1,0\rangle$ to state $|2,0\rangle$. The right-hand drive system produces a destructive quantum interference path, and the system produces photon blockade, as shown in Fig. 5(b). Therefore, the system has excellent chiral quantum optical properties due to photon blockade by right-side driving and photon-induced tunneling by the left-side driving.

5 Conclusions

In summary, we studied a precisely controlled spinning microresonator driven by a weak field. By adjusting the coupling strength between modes and the detuning amount of the light field, asymmetric photon statistics are generated even under the weaker nonlinear Kerr term. Due to chiral light-matter interactions, the destructive quantum interference generated in the right side drive prevents the nonresonant transition path of state $|1,0\rangle$ to state $|2,0\rangle$, so photon blockade can only be generated by driving the spinning resonator on right side but not from the left side that drives the spinning microresonator to generate. Moreover, we can achieve a controllable photon blockade by adjusting the coupling strength between modes and the rotational speed in the chiral interaction. Our work can be applied to chiral optics, single photon sources and nonreciprocal quantum communication.

Acknowledgements We would like to thank the support from the National Natural Science Foundation of China under Grant Nos. 62071064 and 62131002, the Fundamental Research Funds for the Central Universities of China under Grant No. 2019XD-A02, and the Fund of State Key Laboratory of Information Photonics and Optical Communications (Beijing University of Posts and Telecommunications) (No. IPOC2022ZT10), China.

References

1. D. R. Yennie, Integral quantum Hall effect for nonspecialists, *Rev. Mod. Phys.* 59(3), 781 (1987)
2. M. König, S. Wiedmann, C. Brüne, A. Roth, H. Buhmann, L. W. Molenkamp, X. L. Qi, and S. C. Zhang, Quantum spin Hall insulator state in HgTe quantum wells, *Science* 318(5851), 766 (2007)
3. Y. X. Zhao, Equivariant *PT*-symmetric real Chern insulators, *Front. Phys.* 15(1), 13603 (2020)
4. I. Serban, B. Béri, A. R. Akhmerov, and C. W. J. Beenakker, Domain wall in a chiral p-wave superconductor: A pathway for electrical current, *Phys. Rev. Lett.* 104(14), 147001 (2010)
5. C. Junge, D. O'Shea, J. Volz, and A. Rauschenbeutel, Strong coupling between single atoms and nontransversal photons, *Phys. Rev. Lett.* 110(21), 213604 (2013)
6. I. Shomroni, S. Rosenblum, Y. Lovsky, O. Bechler, G. Guendelman, and B. Dayan, All-optical routing of single photons by a one-atom switch controlled by a single photon, *Science* 345(6199), 903 (2014)
7. R. Mitsch, C. Sayrin, B. Albrecht, P. Schneeweiss, and A. Rauschenbeutel, Quantum state-controlled directional spontaneous emission of photons into a nanophotonic waveguide, *Nat. Commun.* 5(1), 5713 (2014)
8. X. F. Liu, T. J. Wang, Y. P. Gao, C. Cao, and C. Wang, Chiral microresonator assisted by Rydberg-atom ensembles, *Phys. Rev. A* 98(3), 033824 (2018)
9. I. J. Luxmoore, N. A. Wasley, A. J. Ramsay, A. C. T. Thijssen, R. Oulton, M. Hugues, S. Kasture, V. G. Achanta, A. M. Fox, and M. S. Skolnick, Interfacing spins in an InGaAs quantum dot to a semiconductor waveguide circuit using emitted photons, *Phys. Rev. Lett.* 110(3), 037402 (2013)
10. D. Holzmann, M. Sonnleitner, and H. Ritsch, Self-ordering and collective dynamics of transversely illuminated pointscatterers in a 1D trap, *Eur. Phys. J. D* 68(11), 352 (2014)
11. Q. W. Shi, Z. F. Wang, Q. X. Li, and J. L. Yang, Chiral selective tunneling induced graphene nanoribbon switch, *Front. Phys. China* 4(3), 373 (2009)
12. P. Lodahl, S. Mahmoodian, S. Stobbe, A. Rauschenbeutel, P. Schneeweiss, J. Volz, H. Pichler, and P. Zoller, Chiral quantum optics, *Nature* 541(7638), 473 (2017)
13. H. J. Kimble, Strong interactions of single atoms and photons in cavity QED, *Phys. Scr.* T76(1), 127 (1998)
14. X. W. Xu, H. Q. Shi, and A. X. Chen, Nonreciprocal transition between two indirectly coupled energy levels, *Front. Phys.* 17(4), 42505 (2022)
15. K. Y. Bliokh, F. J. Rodríguez-Fortuño, F. Nori, and A. V. Zayats, Spin–orbit interactions of light, *Nat. Photonics* 9(12), 796 (2015)
16. A. Aiello, P. Banzer, M. Neugebauer, and G. Leuchs, From transverse angular momentum to photonic wheels, *Nat. Photonics* 9(12), 789 (2015)
17. K. Y. Bliokh and F. Nori, Transverse and longitudinal angular momenta of light, *Phys. Rep.* 592, 1 (2015)
18. Z. Lin, H. Ramezani, T. Eichelkraut, T. Kottos, H. Cao, and D. N. Christodoulides, Unidirectional invisibility induced by *PT*-symmetric periodic structures, *Phys.*

Rev. Lett. 106(21), 213901 (2011)
19. L. Chang, X. Jiang, S. Hua, C. Yang, J. Wen, L. Jiang, G. Li, G. Wang, and M. Xiao, Parity-time symmetry and variable optical isolation in active-passive-coupled microresonators, *Nat. Photonics* 8(7), 524 (2014)
20. Y. Y. Fu, Y. D. Xu, and H. Y. Chen, Negative refraction based on purely imaginary metamaterials, *Front. Phys.* 13(4), 134206 (2018)
21. A. Imamoğlu, H. Schmidt, G. Woods, and M. Deutsch, Strongly interacting photons in a nonlinear cavity, *Phys. Rev. Lett.* 79(8), 1467 (1997)
22. J. Q. Liao and C. Law, Correlated two-photon transport in a one-dimensional waveguide side-coupled to a nonlinear cavity, *Phys. Rev. A* 82(5), 053836 (2010)
23. A. Miranowicz, M. Paprzycka, Y. X. Liu, J. Bajer, and F. Nori, Two-photon and three-photon blockades in driven nonlinear systems, *Phys. Rev. A* 87(2), 023809 (2013)
24. Y. P. Gao, X. F. Liu, T. J. Wang, C. Cao, and C. Wang, Photon excitation and photon-blockade effects in optomagnonic microcavities, *Phys. Rev. A* 100(4), 043831 (2019)
25. W. L. Xu, Y. P. Gao, T. J. Wang, and C. Wang, Magnon-induced optical high-order sideband generation in hybrid atom-cavity optomagnonical system, *Opt. Express* 28(15), 22334 (2020)
26. K. Wang, Y. P. Gao, R. Jiao, and C. Wang, Recent progress on optomagnetic coupling and optical manipulation based on cavity-optomagnonics, *Front. Phys.* 17(4), 42201 (2022)
27. Y. P. Gao and C. Wang, Hybrid coupling optomechanical assisted nonreciprocal photon blockade, *Opt. Express* 29(16), 25161 (2021)
28. P. Rabl, Photon blockade effect in optomechanical systems, *Phys. Rev. Lett.* 107(6), 063601 (2011)
29. A. Nunnenkamp, K. Børkje, and S. M. Girvin, Single-photon optomechanics, *Phys. Rev. Lett.* 107(6), 063602 (2011)
30. X. B. Yan, H. L. Lu, F. Gao, F. Gao, and L. Yang, Perfect optical nonreciprocity in a double-cavity optomechanical system, *Front. Phys.* 14(5), 52601 (2019)
31. D. Armani, T. Kippenberg, S. Spillane, and K. Vahala, Ultra-high-Q toroid microcavity on a chip, *Nature* 421(6926), 925 (2003)
32. B. Dayan, A. S. Parkins, T. Aoki, E. P. Ostby, K. J. Vahala, and H. J. Kimble, A photon turnstile dynamically regulated by one atom, *Science* 319(5866), 1062 (2008)
33. V. Braginsky, M. Gorodetsky, and V. Ilchenko, Quality factor and nonlinear properties of optical whispering gallery modes, *Phys. Lett. A* 137(7-8), 393 (1989)
34. T. Carmon, L. Yang, and K. J. Vahala, Dynamical thermal behavior and thermal self-stability of microcavities, *Opt. Express* 12(20), 4742 (2004)
35. K. Totsuka and M. Tomita, Optical microsphere amplification system, *Opt. Lett.* 32(21), 3197 (2007)
36. Y. S. Park and H. Wang, Resolved-sideband and cryogenic cooling of an optomechanical resonator, *Nat. Phys.* 5(7), 489 (2009)
37. S. Weis, R. Rivière, S. Deléglise, E. Gavartin, O. Arcizet, A. Schliesser, and T. J. Kippenberg, Optomechanically induced transparency, *Science* 330(6010), 1520 (2010)
38. T. Carmon, H. Rokhsari, L. Yang, T. J. Kippenberg, and K. J. Vahala, Temporal behavior of radiation-pressure-induced vibrations of an optical microcavity phonon mode, *Phys. Rev. Lett.* 94(22), 223902 (2005)
39. F. Monifi, J. Zhang, K. Ozdemir, B. Peng, Y. Liu, F. Bo, F. Nori, and L. Yang, Optomechanically induced stochastic resonance and chaos transfer between optical fields, *Nat. Photonics* 10(6), 399 (2016)
40. Y. P. Gao, C. Cao, P. F. Lu, and C. Wang, Phase-controlled photon blockade in optomechanical systems, *Fundamental Research* (2022) (in press)
41. Y. W. Hu, Y. F. Xiao, Y. C. Liu, and Q. Gong, Optomechanical sensing with on-chip microcavities, *Front. Phys.* 8(5), 475 (2013)
42. T. J. Kippenberg, R. Holzwarth, and S. A. Diddams, Microresonator-based optical frequency combs, *Science* 332(6029), 555 (2011)
43. F. Bo, J. Wang, J. Cui, S. K. Ozdemir, Y. Kong, G. Zhang, J. Xu, and L. Yang, Lithium-niobate–silica hybrid whispering-gallery-mode resonators, *Adv. Mater.* 27(48), 8075 (2015)
44. Q. T. Cao, H. Wang, C. H. Dong, H. Jing, R. S. Liu, X. Chen, L. Ge, Q. Gong, and Y. F. Xiao, Experimental demonstration of spontaneous chirality in a nonlinear microresonator, *Phys. Rev. Lett.* 118(3), 033901 (2017)
45. B. Peng, S. K. Ozdemir, F. Lei, F. Monifi, M. Gianfreda, G. L. Long, S. Fan, F. Nori, C. M. Bender, and L. Yang, Parity-time-symmetric whispering-gallery microcavities, *Nat. Phys.* 10(5), 394 (2014)
46. L. Feng, Z. J. Wong, R. M. Ma, Y. Wang, and X. Zhang, Single-mode laser by parity-time symmetry breaking, *Science* 346(6212), 972 (2014)
47. H. Hodaei, M. A. Miri, M. Heinrich, D. N. Christodoulides, and M. Khajavikhan, Parity-time-symmetric microring lasers, *Science* 346(6212), 975 (2014)
48. S. M. Spillane, T. J. Kippenberg, K. J. Vahala, K. W. Goh, E. Wilcut, and H. J. Kimble, Ultrahigh-Q toroidal microresonators for cavity quantum electrodynamics, *Phys. Rev. A* 71(1), 013817 (2005)
49. H. Wang, Multi-peak solitons in PT-symmetric Bessel optical lattices with defects, *Front. Phys.* 11(5), 114204 (2016)
50. J. Zhu, S. K. Ozdemir, Y. Xiao, L. Li, L. He, D. Chen, and L. Yang, On-chip single nanoparticle detection and sizing by mode splitting in an ultrahigh-Q microresonator, *Nat. Photonics* 30(2), 4,46 (2010)
51. Y. Zhi, X. C. Yu, Q. Gong, L. Yang, and Y. F. Xiao, Single nanoparticle detection using optical microcavities, *Adv. Mater.* 29(12), 1604920 (2017)
52. T. Reynolds, N. Riesen, A. Meldrum, X. Fan, J. M. M. Hall, T. M. Monro, and A. François, Fluorescent and lasing whispering gallery mode microresonators for sensing applications, *Laser Photonics Rev.* 11(2), 1600265 (2017)
53. L. X. Zhang, R. Zhang, and Z. Q. Li, Study on a vapor sensor based on the optical properties of porous silicon microcavities, *Front. Phys. China* 2(2), 166 (2007)
54. S. Maayani, R. Dahan, Y. Kligerman, E. Moses, A. U.

Hassan, H. Jing, F. Nori, D. N. Christodoulides, and T. Carmon, Flying couplers above spinning resonators generate irreversible refraction, *Nature* 558(7711), 569 (2018)

55. R. Huang, A. Miranowicz, J. Q. Liao, F. Nori, and H. Jing, Nonreciprocal photon blockade, *Phys. Rev. Lett.* 121(15), 153601 (2018)
56. Y. Jiang, S. Maayani, T. Carmon, F. Nori, and H. Jing, Nonreciprocal phonon laser, *Phys. Rev. Appl.* 10(6), 064037 (2018)
57. H. Jing, H. Lü, S. Özdemir, T. Carmon, and F. Nori, Nanoparticle sensing with a spinning resonator, *Optica* 5(11), 1424 (2018)
58. B. Li, R. Huang, X. Xu, A. Miranowicz, and H. Jing, Nonreciprocal unconventional photon blockade in a spinning optomechanical system, *Photon. Res.* 7(6), 630 (2019)
59. G. B. Malykin, The Sagnac effect: Correct and incorrect explanations, *Phys. Uspekhi* 43(12), 1229 (2000)
60. T. C. H. Liew and V. Savona, Single photons from coupled quantum modes, *Phys. Rev. Lett.* 104(18), 183601 (2010)
61. M. Bamba, A. Imamoğlu, I. Carusotto, and C. Ciuti, Origin of strong photon antibunching in weakly nonlinear photonic molecules, *Phys. Rev. A* 83(2), 021802 (2011)